Journal of Harbin Engineering University
ISSN: 1006-7043

Vol 46 No. 12
December 2025

Biomedical and Optical Applications of Nanostructured Yttrium orthovanadate (YVO_4) Material

S. Devi[1]*, E. Kavitha[2], C. Andal[3], D. Preethi[4]

[1]*Research Scholar, Department of Physics, Dr. M.G.R. Educational and Research Institute, Chennai-600095, Tamil Nadu, India.

[2]Professor, Department of Physics, Dr. M.G.R. Educational and Research Institute, Chennai-600095, Tamil Nadu, India.

[3]Professor, Department of Physics, Dr. M.G.R. Educational and Research Institute, Chennai-600095, Tamil Nadu, India.

[4]Research Scholar, Department of Physics, Dr. M.G.R. Educational and Research Institute, Chennai-600095, Tamil Nadu, India.

Abstract - Recently, the well grown level of nanotechnology in various fields, the synthesis of nanoparticles was effectively carried out on Yttrium orthovanadate (YVO_4) using a microwave-assisted technique with suitable temperature. Various microscopic and spectroscopic methods, including XRD, SEM, FTIR, UV, and PL were employed to characterize physical, chemical and optical properties of synthesized YVO_4. The XRD results revealed purity of nanostructured YVO_4 material. The SEM study discovered a highly porous, rough and irregular agglomerated surface morphology, suggesting the formation of YVO_4 nanoparticles. Also, FT-IR analysis verified the presence of Y-O and VO_4, indicating the formation of YVO_4. Also optical properties from photoluminescence spectrum and UV–vis-NIR studies were carried out for its potential of optical applications. Additionally, TGA was used to assess thermal properties for the determination of thermal stability. The antibacterial characteristics were assessed using the agar method with *S. aureus, E. coli,* and human fungal pathogens like *C. albicans*. The results were favourable owing to synergetic effect of vanadium and yttrium, with yttrium ions enhancing structural stability and surface properties, which further enhanced antibacterial and antifungal activities. These findings suggest that microwave-assisted synthesis of YVO_4 nanoparticles is effective for antimicrobial purposes and can be utilized in the biological industry.

Keywords: PXRD; SEM;FTIR; UV; PL; Anti-microbial activity.

1.

Introduction

Recent research has extensively focused on novel nanomaterials, such as nanoparticles (NPs), using various methodologies for comprehensive applications [1]. Since NPs exhibit numerous physical properties, which are essential in the field of optoelectronics for the development of various devices including laser diodes, light-emitting diodes (LEDs), display panels and photodetectors. Different types of nanoparticles (NPs) demonstrate enhanced photoluminescence (PL) energy transfer efficiency and tunable spectral properties, which contribute to the advancement of materials in optoelectronic and photonic research. In another context, various types of NPs are utilized in biological research since their ability to facilitate the attachment of multiple biomolecules [2]. NPs are predominantly classified into several categories, including carbon-based materials, polymer-based composite NPs, biomolecule-derived NPs, and inorganic metal or metal oxide-based nanomaterials [3]. Inorganic metal-based NPs are particularly significant in various research sectors because of their exceptional stability, tunable optical properties, magnetic behavior, and biocompatibility [4]. Furthermore, these

nanoparticles exhibit significant potential foroptoelectronic and biomedical applications [5]. In the optoelectronic field, nanoparticles introduce surface defects and new electronic levels within the bandgap, thereby enhancing photoluminescence properties [6]. Additionally, their nanoscale size allows for strong interactions with photons, resulting in unique absorption, scattering, and emission characteristics [7]. This makes them excellent materials for the development of photodetectors, solar cells, and bio imaging applications [8].

In the biomedical industry, these nanoparticles demonstrate notable performance through multifaceted mechanisms of action, which includes membrane disruption, Reactive Oxygen Species (ROS) generation, and binding to intracellular components [9]. The biomedical application of NPs has garnered significant interest in the management of various bacterial and fungal infections. The increasing prevalence of microbial organisms that have developed resistance to several conventional antibiotics necessitates in the progress of unique bactericidal agents, as this resistance imposes a significant burden on healthcare economies [10].

Yttrium orthovanadate (YVO_4) is an important rare earth material that has garnered significant attention owing to its crystalline structure and favourable luminescent nature of high chemical stability with low energy of phonon [11]. In addition, it is considered an important host materials in rare earth elements due to their excellent thermal, optical and electrical conductivities [12]. The excellent optical performance of YVO_4 contributes to enhancing the antibacterial activity by reducing the band gap, which is capable of generating Reactive Oxygen Species (ROS) that easily damage cell wall proteins and DNA [13]. Recent research has concluded that YVO_4 exhibits antibacterial properties, particularly in addressing the challenge of increasing the number of multidrug-resistant pathogens. Antibacterial activity is used to treat bacterial infections by killing or inhibiting the growth of bacteria and prevents infection on medical devices and wound dressings. Antibacterial activity is related to compounds that locally kill bacteria or slow down their growth, without being in general toxic to surrounding tissue [14].

In this paper, we have reported our investigation results of synthesized nanostructured YVO_4 material is shown. The characterization of YVO_4 is a crucial component of this research, as it is essential for determining the morphological features, crystallinity, thermal stability and optical properties, including the band gap and transmittance using the techniques employed included XRD, SEM, EDAX, FT-IR, UV, PL spectroscopy and TG/DTA. Moreover, we assessed the biological activity of the materials in case of two bacterial strains, *S. aureus* and *E. coli*, and one fungal strain, *C. albicans*, using the standard agar diffusion method.

2. Materials and Methods

2.1 Materials

Yttrium Nitrate hexahydrate [$Y(NO_3)_36H_2O$, 99.9% pure], ammonium metavanadate [NH_4VO_3], and sodium hydroxide pellets [NaOH, 98% pure] was obtained from SRL (India) and used without further treatment or purification for the synthesis of YVO_4. The entire synthesis procedure was conducted using distilled water as solvent.

2.2 Synthesis of YVO_4

Microwave-assisted method is the best method. Also, the microwave-assisted synthesis method resulted in smaller nanoparticles compared to the conventional approach. This is attributed to the fact that microwave heating facilitates rapid nucleation, which is advantageous for producing smaller and more uniform nanostructures in the final product [15].Yttrium nitrate hexahydrate [$Y(NO_3)_3{\cdot}6H_2O$] and ammonium metavanadate [NH_4VO_3] were dissolved in 100 mL of distilled water in the concentrations of 1 molar ratio and was stirred continuously until a transparent solution was obtained. Subsequently, sodium hydroxide (NaOH) pellets were added to the solution with 1:1 ration of concentration. After vigorous stirring for one hour, a white precipitate was formed. The precipitate was then neutralized to pH of 10 using NaOH. The solution was subjected to microwave treatment at 700 W for 15 m. The specimen was thoroughly dried and filtered

using Whatmann filter paper which was washed multiple times using distilled water. An annealing process of this white precipitate was conducted in the muffle furnace at 650 °C for two hrs. Finally, the resulting samples were ground using a mortar and were collected for further characterization studies. The image of synthesized nanostructured YVO_4 material is shown in Fig.1

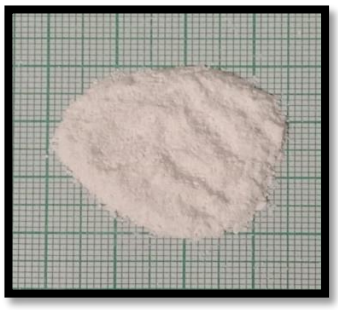

Fig. 1 Image of YVO_4powder sample

3. Results and Discussions

3.1 X – Ray Diffraction Analysis

Powder X Ray Diffraction (PXRD) is ageneral non-destructive characterisation technique. It provides an important information about the purity, phase nature and lattice parameters in the quantitative analysis [16]. The crystalline character of YVO_4 was found using Powder X-ray diffraction spectroscopy (XRD, which was obtained from the instrument X' Pert PRO – PANalytical of Cu Kαradiation with spectral range 10 ° to 80 ° at a speed of 5°/min. Fig.2 shows the X-Ray Diffraction of the synthesized YVO_4, which reveals several sharp diffraction peaks at the angle of 18.5°, 24.7°, 33.3°, 35.4°, 40.4°, 44.8°, 49.6° and 51.1° with corresponding (h k l) value of (1 0 1), (2 0 0), (1 1 2), (2 2 0), (3 0 1), (1 0 3), (3 1 2) and (4 0 0) planes, respectively with the reference of JCPDS file 17-0341 [17] and it is identified the tetragonal zircon crystalline phase of YVO_4.

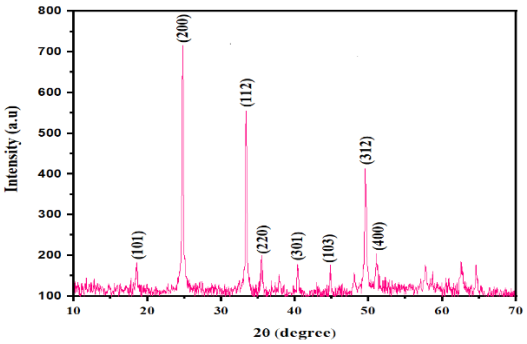

Fig. 2 XRD pattern of the synthesized YVO_4

3.2 Morphological Analyses

3.2.1 Scanning Electron Microscope (SEM) studies

Scanning electron microscopy is an effective imaging method, to produce surface details with high resolution images. This technique is an indispensable tool for exploring vast range of applications in nanomaterials [18]. Fig.3 shows the SEM image of the synthesized YVO_4, it reveals that the uniform semi – cylindrical domains were observed. It is due to the cluster of nanoparticles with size 113 nm and the determined average particle surface area size was 120 nm. The formation of slight elongation in its size was seen between 113.0 nm to 138.8nm. These values suggest a moderately narrow size distribution of YVO_4, which was influenced by the agglomerated NPs [19]. Since, the usage of NaOH not only maintains the pH but also provides less agglomerated Yttrium orthovanadate particles. The rough surface and permeable nature of NPs are advantageous for enhancing surface-active sites, which are useful for diverse applications, such as antibacterial and catalytic performance.

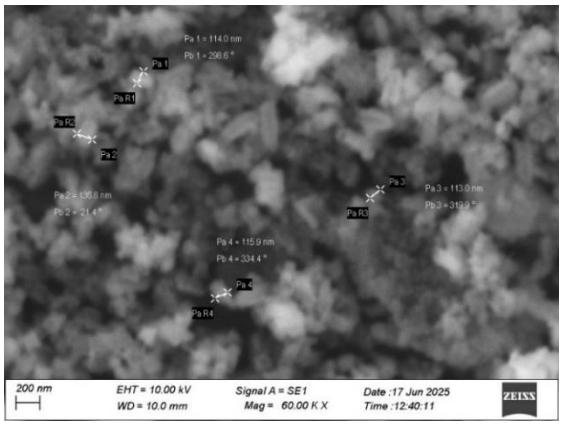

Fig. 3 SEM image of YVO_4

3.2.2 Energy - Dispersive X-ray Analysis (EDAX) analysis

Energy - Dispersive X-rayAnalysis(EDAX) is an essential technique which establish the basic information about the elemental composition analysis [20].The Fig.4 shows the presence of required elements in YVO_4 which were analysed using Energy-Dispersive X-ray Analysis (EDAX, Oxford Instrument).

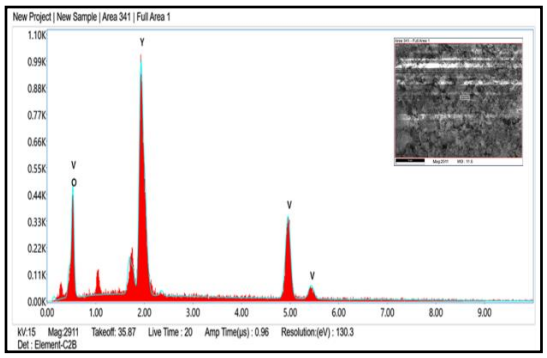

Fig. 4 EDAX analysis of YVO_4

The EDAX spectrum of YVO_4 confirm that YVO_4 is chemically composed of Y, V, and O, with no detectable impurities. The atomic weight compositions (%) of the elements in the K shell were 18.22, 23.47, and 58.31% for Y, V, and O, respectively. The results obtained confirm the stoichiometric ratio of YVO_4 as 1:1:4.

3.2.3 FTIR Analysis

FT – Raman analysis provides the detailed information about the various functional groups present in the compound. It is a molecular spectrum, hence it reveals the molecular band structure of the micro and macro molecules [21]. The YVO_4 was characterized using Fourier Transform Infrared Spectroscopy (FT-IR, Perkin Elmer, Spectrum Two) in spectral range of 400 - 4000 cm^{-1}, with a scan speed of 20 nm/min. The type and range of band intensities are critical factors, as they provide insights into whether the structure is crystalline or amorphous [22].The spectrum is shown in the Fig.5.The asymmetric (tetrahedral) and symmetric V-O stretching vibrations of VO_4^{3-} were found at 1020 cm^{-1} and 819 cm^{-1}. In addition, the Y-O or VO_4 bending vibration band (lattice mode) was observed at 492 cm^{-1}. The bands serve as evidence for the formation of YVO_4 and the other vibrational modes of V-O and Y-O bonds within the perovskite structure, aiding in the identification of the material and confirming its composition or any structural alterations. Furthermore, the broad band at approximately 3428 cm^{-1} is indicative of O-H stretching vibrations, while another broad band at 1639 cm^{-1} belongs to H-O-H bending vibrations. These findings are consistent with EDAX studies.

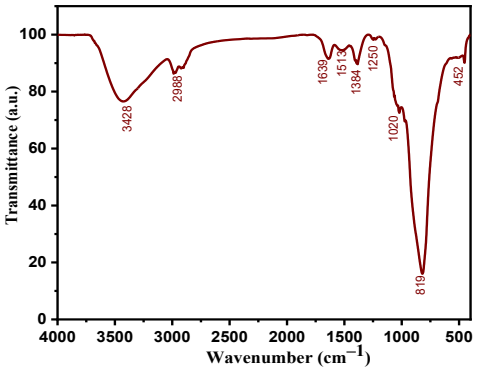

Fig. 5 FT-IR spectrum of YVO_4

3.3. Optical Studies

3.3.1 UV-Vis-NIR Analysis

UV – Vis spectrum offers the information about the materials reaction to its absorption in a particular wavelength. This method is frequently

applied to discover the potency, identification and purity of different materials [23].The optical properties, including absorption and transmission behaviors, were determined using UV-Vis spectroscopy within the wavelength range of 200-1200 nm range (Perkin-Elmer Lambda 35 spectrophotometer, 100 nm/min^{-1} scan speed, 1 nm spectral bandwidth). Fig. 6 (a) shows the UV-absorbance spectrum of YVO_4, which is characterized by a broad peak at ~ 372 nm. This peak is likely attributable to an electronic transition between d band and p band, specifically from vanadium and yttrium atoms [24].

Fig. 6 (b) shows the UV-Transmittance spectra of the materials. It demonstrates low transparency within the 400 nm range, confirming strong absorption between 200-400 nm due to the p-d electronic transition [25]. As the wavelength increased, the transmittance also increased in the visible-NIR region. Moreover, increased transparency results in stronger emissions, which consequently reduces the re-absorption of emitted light. This characteristic is advantageous for the development of optoelectronic devices [26]. These highly transparent materials are recognized as hosts for a range of luminescent converters. Furthermore, increased transparency contributes to enhanced antibacterial activity, as the material is clean and effectively inhibits bacterial growth [27].

Using UV absorbance and transmittance spectrum, the bandgap was calculated using a Tauc plot from the UV-Vis absorption spectrum [28]. The equation is

$$(\alpha h\nu)^{1/n} = A\,(h\nu - E_g) \quad (1)$$

Here, hv is the photon energy, α is the absorption coefficient, E_g is the optical band gap, A is a proportionality constant, and n is Tauc exponent, which depends on the type of band gap:

n = 1/2 for a direct band gap and n = 2 for an indirect band gap. The graph Fig.6 (c)was plotted against (αhv) versus energy and the obtained value was 3.2 eV is in consistent with earlier reported [29]. This direct band gap graph confirms the semiconducting nature of YVO_4 [30]. The wide bandgap facilitates ultraviolet and visible light emission, rendering it suitable for applications in photo electronic devices [31]. Furthermore, the band gap is pertinent to antibacterial studies, as a higher band gap facilitates the formation of electron-hole pairs that readily react with oxygen to generate Reactive Oxygen Species (ROS), which eradicates bacteria on surfaces [32].

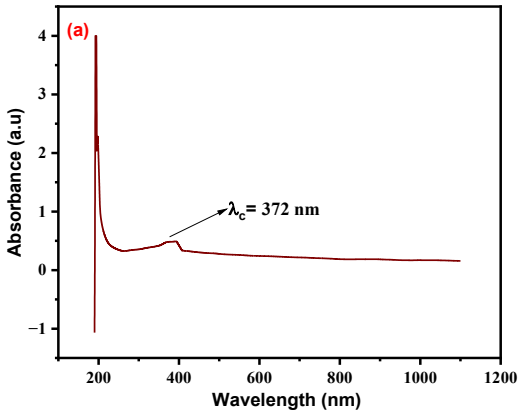

Fig. 6 (a) UV Absorbance of YVO_4

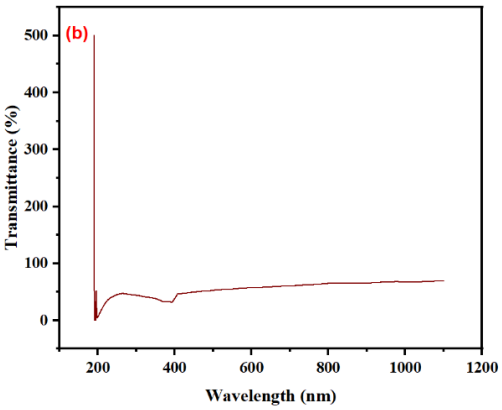

Fig. 6 (b) Transmittance spectra of YVO_4

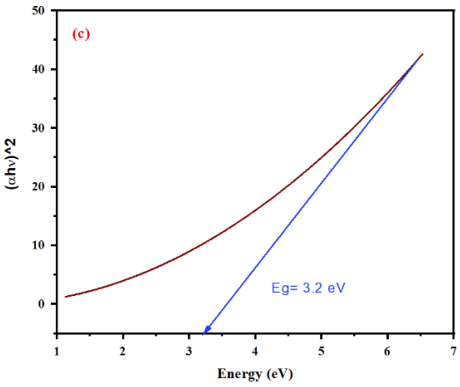

Fig. 6 (c) Band gap determination graph of YVO_4

3.3.2 Photoluminescence (PL)

Photoluminescence is a well-known effective technique used broadly to find the different impurities present in the substances and it has various applications in both optical science and technology. This emission spectrum is very much useful to identify the surface impurity level and interface roughness [33]. The PL spectrum of YVO_4 is presented in Fig.7. There are three emission peaks were identified at 409 (blue) nm, 573 (yellow) nm, and 627 (red) nm. The first peak at 409 nm reveals to the near-band-edge PL peak, which is attributed to charge transfer within the VO_4^{2-} tetrahedral groups. This transition involves the movement from oxygen 2p orbital to vanadium 3p orbital through radiative recombination. Beyond 400 nm, the YVO_4 nanoparticles exhibits an intrinsic charge-transfer of emissions within (VO_4^{3-}) groups, such exhibited energies being presented with the energy gap [34].

This emission further substantiates the role of the host lattice in the PL response of YVO_4. The yellow emission (573 nm) was associated with the oxygen vacancies present in VO_4^{2-} . While the red emission at 627 nm signifies deep-level V-related defects. These PL spectra confirm that the material possesses optical properties which are suitable for OLED applications and also due to 409 nm near-band edge and luminescence pathway, also beneficial for photocatalytic process and bio imaging applications [35].

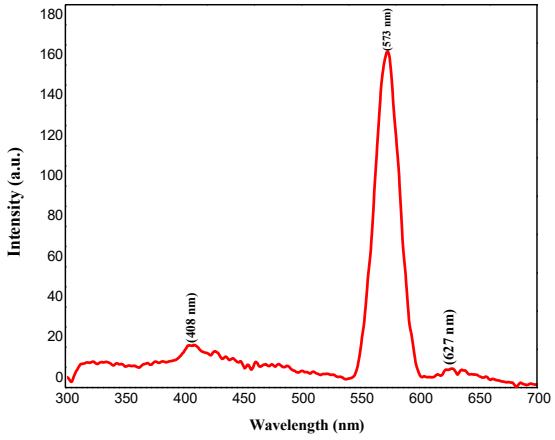

Fig. 7 Represents the PL spectrum of the YVO_4

3.4 Thermogravimetric and Differential Thermal Analyses (TG/DTA)

In general TGA, is employed to examine the temperature degradation, content of absorbed moisture and decomposition state. In DTA, the temperature variation between the specimen and inner substances is analysed as the function of applied temperature [36]. The thermal stability of the material was analyzed using the TGA, SII Nanotechnology Inc., Japan, EXSTAR6200 TG/DTA, and Perkin Elmer, TGA 4000. The TGA and DTA curves of YVO_4 are presented in Fig.8.In TGA curve there are three distinct stages of weight loss were observed at 101 °C, 350 °C and 585 °C temperature the initial stage, which occurred below 100 °C, indicated the desorption of water molecules and the next gradual weight loss, observed between 100 °C to 350 °C, suggests the removal of additional impurities, such as nitrate or hydroxyl moieties. From the range of 350 °C to 500 °C, only a minor weight loss (5.2 %) was recorded [37] demonstrating the excellent thermal stability of YVO_4. At 210°C, gradually weight loss was observed at 97 mg and then even at 600 °C, the material remained stable, confirming its suitability for high-temperature applications, such as photonics and antibacterial coatings. The DTA curve reveals the presence of minor endothermic peak between 51 °C to 55 °C is an indicative of the evaporation of absorbed water molecules in the synthesis process. Also above 100 °C corresponds to the decomposition of the initial material moieties, such as nitrate and carbonyl sources.

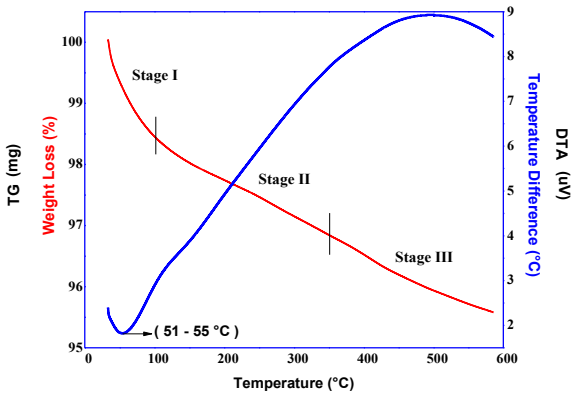

Fig. 8 TG/DTA curve of YVO_4

The overall findings from the TGA and DTA analyses indicate that YVO_4 exhibit excellent thermal stability, making it suitable for various applications. This is because thermal resistance is crucial in numerous fields of research. Furthermore, the enhanced thermal stability significantly improved the PL properties of YVO_4. This is attributed to the stabilization of defect states, reduction of quenching, and preservation of both the surface and crystal structures [38].

3.5 Biological Evaluation

Antibacterial activity is an essential tool in nanomaterial's medicinal applications. It represents the chemical which limits or completely destroy the growth of bacteria in a particular level despite being non-toxic to the enclosing region. Also this activity, reveals the ability of the substances to the zone of inhibition [39]. The antibacterial and antifungal properties of YVO_4 were evaluated using the agar disk diffusion method [40].Before this experimental procedure, bacterial cultures were maintained on nutrient agar medium and fungal cultures were maintained on potato dextrose agar (PDA) medium. The YVO_4 samples were prepared at a concentration of 100 µg mL – in methanol. The test microorganisms was inoculated inside the respective medium by the spread plate method, using 10 µL of a 10 cells/mL suspension, with 24-hour cultures of bacterial growth in nutrient broth. Subsequent to solidification, filter paper wells with a diameter of 5 mm, impregnated with the extracts, was laid down on the plates inoculated with the test organisms. Amoxicillin (10 µg) was utilised as the standard antibacterial agent. The antibacterial assay plates was incubated at 37°C for 24 h. The diameters of the inhibition zones was measured in millimetres, and the antifungal properties was analysed. Potato dextrose agar plates was inoculated with each fungal culture, which was 10 days old, using point inoculation. Filter paper wells, each with a diameter of 5 mm and impregnated with 100 µg of the synthesized YVO_4 NPs, was deposited in the plates seeded with the test organisms. Fluconazole, at a concentration of 10 µg per well, served as the positive control. The antimicrobial activity was assessed after 72 h of incubation at 28°C, and the diameters of the inhibition zones were measured in millimetres [41,42].

In this study, we evaluated the antibacterial and antifungal properties against the Gram-positive bacterium S. aureus, the Gram-negative bacterium E. coli, and the fungus *C. albicans* using the agar well diffusion method. Fig.9 (a) and (b) represent the antibacterial study plates containing *S. aureus* and *E. coli*. At where, amoxicillin was used as the standard reference. Upon increasing the concentration of YVO_4, an enhancement in the incubation zone was observed. Using these images, we calculated the Zone of Inhibition (ZOI), with the results depicted in the bar diagram in Fig.9 (c) and (d).At a maximum concentration of 30 µL, the inhibition zones measured 16 mm and 18 mm for *S. aureus* and *E. coli,* respectively, indicating effective results. Fig.10 (a) illustrates the antifungal study conducted on a plate with *C. albicans* present. The results indicated that increasing the concentration of the material enhanced the zone of inhibition, suggesting that the material is an optimal antifungal agent against *C. albicans*. Fluconazole was used as the reference drug in this study.

Table 1. Antibacterial activity data of YVO_4

S.No	**Pathogenic bacteria**	**Zone of inhibition (mm)**			**Standard (Amoxicillin)**
		10	**20**	**30**	
1.	*Staphylococcus aureus*	05	09	16	22
2.	*E. coli*	05	11	18	22

Table 2. Antifungal activity data of YVO_4

S.No	Pathogenic Fungi	Zone of inhibition (mm)			Standard (Fluconazole)
		10 µg	20 µg	30 µg	
1.	*Candida albicans*	05	09	12	18

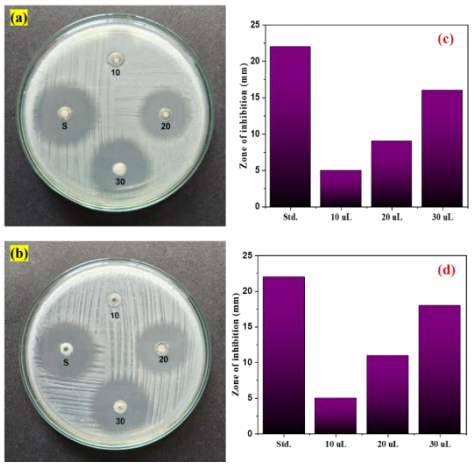

Fig. 9 Images of *(a) S. aures* and (b) *E. coli*and Zone of inhibition of

(c) *S. aures* and (d) *E. coli*

The experiment was conducted in triplicates (n=3). A zone of inhibition bar diagram is shown in Fig.10 (b). The maximum Zone Of Inhibition (ZOI) of 12 mm was observed when 30 µL of the material was used. This mechanism involves photodynamic effects, wherein the materials generate Reactive Oxygen Species (ROS) upon exposure to light, which subsequently damage the cell wall and effectively kill bacteria and fungi, which significantly contribute to the antibacterial properties of the material by promoting the overall findings indicate that the synthesized material functions as an effective antibacterial and antifungal agent.

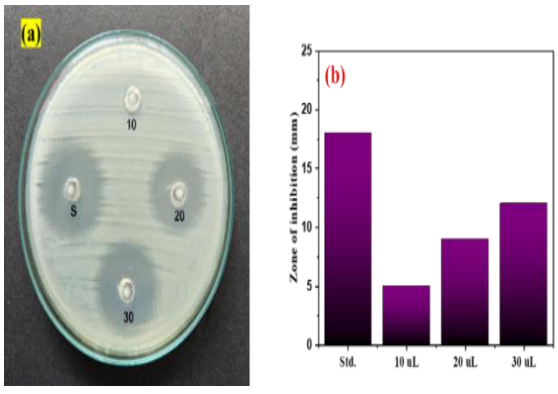

Fig. 10Antifungal activity of

(a) *C. albicans* (b) zone of inhibition

4. Conclusion

In this study, we successfully synthesized YVO_4 using a time-efficient and environmental friendly microwave-assisted method. The tetragonal crystallinity nature of the compound was retained and it was confirmed by powder XRD. The uniform semi cylindrical domain image were confirmed by SEM analysis. The presence of VO_4^{2-} functional groups in YVO_4 was confirmed by FT-IR analysis. The presence of vanadium (V), yttrium (Y), and oxygen (O), along with their correct stoichiometric composition (1:1:4), was successfully assessed using EDAX. The UV-vis NIR spectrum of absorbance at 372 nm was observed in broad peak and the energy gap calculated value was 3.2 eV. The material demonstrated good thermal stability, even at elevated temperatures, as confirmed by TG/DTA studies. The biological evaluation of the compound illustrates that the increasing concentration of the material enhanced the zone of inhibition. It is concluded that the material is an optimal antifungal agent against *Candida albicans.* Moreover, the antibacterial and antifungal evaluation results showed an improved ZOI owing to the material's ability to readily interact with the bacterial cell wall, leading to the destruction of bacteria and fungi. With the continuous increase in bacterial resistance to existing antibiotics, it is crucial to discover new antimicrobial sources toaddress this global public health issue. The potential optical application of YVO_4 is confirmed with PL studies for OLED device applications.

Reference

1. Elkhwaga, A., A. Zidan, A. I. A. A. ElMageed. 2023. Preparation methods of different nanomaterials for various potential applications: A review. Journal of Molecular Structure 1281(C):135148-69.

2. Majeed, M. I., H. N. Bhatti, H. Nawaz, M. Kashif. 2019.In book: Integrating Green Chemistry and Sustainable Engineering. Nanobiotechnology: Applications of nanomaterials in biological research 581-615.

3. Khan, F. A. 2020.In book: Applications of Nanomaterials in Human Health. Nanomaterials: Types, classifications, and

sources.

4. Shen, J.,M. Shafiq,M.Ma,H. Chen. 2020. Synthesis and Surface Engineering of Inorganic Nanomaterials Based on Microfluidic Technology. Nanomaterials 10(6):1177.

5. Kumar, G., C.-C. Lin, H.-C. Kuo, F.-C. Chen. 2024. Enhancing photoluminescence performance of perovskite quantum dots with plasmonic nanoparticles: insights into mechanisms and light-emitting applications. Nanoscale Advances 6(3):782-791.

6. Raizada, P., V. Soni , A. Kumar, P. Singh, A. A. P. Khan, A. M. Asiri, V. K. Thakur, V.-H. Nguyen, G. K. Alqurashi. 2020.Surface defect engineering of metal oxides photocatalyst for energy application and water treatment. Journal of Materiomics 7 (2):388-418.

7. Llka, M., S. Bera, S.-H. Kwon. 2018. Influence of Surface Defects and Size on Photochemical Properties of SnO2 Nanoparticles. Materials 11(6):904-916.

8. Gundepudi,K., P. M. Neelamraju, S. Sangaraju, G. Dalapati, W. B. Ball, S. Ghosh, S. Chakrabortty. 2023. A review on the role of nanotechnology in the development of near-infrared photodetectors: materials, performance metrics, and potential applications. Journal of Materials Science 58(35):1-36.

9. Adeyemi, J., A. O. Oriola, D. Onwudiwe, A.O. Oyedeji. 2022. Plant Extracts Mediated Metal-Based Nanoparticles: Synthesis and Biological Applications. Biomolecules 12 (5):627-655.

10. Fuente, J. M. D. L., V. Grazu. 2012.Nanobiotechnology: Inorganic Nanoparticles vs Organic Nanoparticles. 4:143-153. The Netherlands.

11. Zhang, S., Y. Liang, X. Y. Gao, H.-T. Liu. 2014. Hydrothermal Synthesis and Microstructural, Optical Properties Characterization of YVO_4 Phosphor Powder.Acta Physica Polonica Series a125(1):105-110.

12. Milligan, W.O., L. W. Vernon. 1952. Crystal Structure of Heavy Metal Orthovanadates. The Journal of Physical Chemistry 56 (1):145-147.

13. Talebian, N., S. Amininezhad, M. Doudi. 2013. Controllable synthesis of ZnO nanoparticles and their morphology-dependent antibacterial and optical properties. Journal of Photochemistry and Photobiology B Biology 120C: 66-73.

14. Hajipour, M., K. M. Fromm, A. A. Ashkarran, D. J. D. Aberasturi, I. R. D. Larramendi, T. Rojo, V. Serpooshan, W. J. Parak, M. Mahmoudi. 2012. Antibacterial properties of nanoparticles. Trends in Biotechnology 30(10):499-511.

15. Menon,S. G., R. Krishnan, D. A. K. Bedyal, A. K. Kunti, H. C. Swart, D. Poelman. 2022. Recent advances in microwave synthesis for photoluminescence and photocatalysis. Materials Today Communications 32: 103890.

16. Jun, Z., Wulantuya, DI. Xiao-wei, LIU. Zhi-liang, XU. Gang, XU. Sheng-ming. 2010. Preparation of YVO4:RE (RE=Yb^{3+}/Er^{3+}, Yb^{3+}/Tm^{3+}) nanoparticles via microemulsion-mediated hydrothermal method. Transactions of Nonferrous Metals Society of China 20 (1):231-235.

17. Wong-Ng, W., H.F. McMurdie, C. Hubbard, A. D. Mighell. 2011. JCPDS-ICDD research associateship (Cooperative Program with NBS/NIST). Journal of research of the National Institute of Standards and Technology 106(6):1013.

18. Samuel, H. S., F.-D. M.Ekpan. 2024. The use of Scanning Electron Microscopy SEM for Medical Application: A Mini Review. Eurasian Journal of ScienceEngineering and Technology 4(4):289-294.

19. Xu, Y., H. Li, B. Sun, P. Qiao, L. Ren, G. Tian, B. Jiang, K. Pan, W. Zhou. 2019. Surface Oxygen Vacancy Defect-Promoted Electron-Hole Separation for Porous Defective ZnO Hexagonal Plates and Enhanced Solar-Driven Photocatalytic Performance. Chemical Engineering Journal 379:122295.

20. Abdullah, A., A. Mohammed. 2019. Scanning Electron Microscopy (SEM): A Review. Proceedings of International Conference on HYDRAULICS, PNEUMATICS, SEALING ELEMENTS, TOOLS, PRECISION MECHANICS,

SPECIFIC ELECTRONIC EQUIPMENT & MECHATRONICS.

21. Duval, E. 1992. Far-infrared and Raman vibrational transitions of a solid sphere: Selection rules. Physical review. B Condensed Matter 46(9):5795-5797.

22. Praveena, N. M., P. Shaiju, R. B. A. Raj, B. G. Erathimmanna. 2021. Infrared bands to distinguish amorphous, meso and crystalline phases of poly(lactide)s: Crystallization and phase transition pathways of amorphous, meso and co-crystal phases of poly(L-lactide) in the heating process. Polymer 240 (8):124495.

23. Alaboodi, A.S., S. A. Kadhim, A. Shakir. 2025. Ultraviolet-Visible Spectroscopy, Importance, Principle, Structure and Most Important Applications: A Study Review. International Journal of Novel Research in Physics Chemistry& Mathematics 12 (1):53-60.

24. Kumari, S., S. Paul, S. Raj. 2017. Electronic structure of RVO 3 (R = La and Y): Effect of electron (U) and exchange (J) correlations. Solid State Communications268:20-25.

25. Soumya, K., N. More, M. Choppadandi, D. A. Aishwarya, G. Singh, G. Kapusetti. 2023. A comprehensive review on carbon quantum dots as an effective photosensitizer and drug delivery system for cancer treatment. Biomedical Technology 4:11-20.

26. Stopikowska, N., P. Woźny, M. Suta, T. Zheng, S. Lis, M. Runowski. 2023. Influence of excitation and detection geometry on optical temperature readouts - reabsorption effects in luminescence thermometry. Journal of Materials Chemistry C 11(2).

27. Caixeta, F.J., F. T. Aquino, R. R. Pereira, R. R. Gonçalves. 2021. Highly red luminescent $Nb_2O_5:Eu^{3+}$ nanoparticles in silicate host for solid-state lighting and energy conversion. Optical Materials 111:110671.

28. Parajuli, D., S. Dangi, B. R. Sharma, N. L. Sahu, D. Kc. 2023. Sol-gel synthesis, characterization of ZnO thin films on different substrates, and bandgap calculation by the Tauc plot method. BIBECHANA 20(2):113-125.

29. Kumaravel,V.,A. Suganthi, B.-K. Min, M. Rajarajan, M. Kang. 2014. Designing of YVO4 supported β-Agl nano-photocatalyst with improved stability. RSC Advances 5(1).

30. Mohamed, R. M., F. A. Harraz. 2020. Mechanistic investigation and photocatalytic activity of yttrium vanadate (YVO_4) nanoparticles for organic pollutants mineralization. Journal of Materials Research and Technology 9 (3):5666-5675.

31. Zou, Y., Y. Zhang, Y. Hu, H. Gu. 2018. Ultraviolet Detectors Based on Wide Bandgap Semiconductor Nanowire: A Review. Sensors. 18(7).

32. Yuvaraja, S., V. Khandelwal, X. Tang, X. Li. 2023. Wide bandgap semiconductor-based integrated circuits. Chip 2(5):100072.

33. Gfroerer, T.H. 2006. In book: Encyclopedia of Analytical Chemistry. R.A. Meyers (Ed). 9209-9232.

34. Kolesnikov, I., D. V. Mamonova, M. A. Kurochkin, E. Y. Kolesnikov, E. Lahderanta. 2021. Optical Thermometry by Monitoring Dual Emissions from YVO 4 and Eu3+ in YVO4:Eu3+Nanoparticles. ACS Applied Nano Materials 4 (2):1959-1966.

35. Tiwari, H., S. Singh, R. Kumar, A. Mandal, A. Pathak, N. K. Varma, L. Kumar, V. Gautam. 2025. Novel Advancements in Nanomaterials-Based Contrast Agents Across Multimodal Imaging and Theranostic Applications. Nanoscale Advances7 (21):6753. 36. Kalai, F. E., E. B. Poyraz, C. H. Lai, S. Daoui, P. T. Chelfi, N. Dege, K. Karrouchi, N. Benchat. 2020. Synthesis, spectroscopy, crystal structure, TGA/DTA study, DFT and molecular docking investigations of (E)-4-(4-methylbenzyl)-6-styrylpyridazin-3(2H)-one. Journal of Molecular Structure 1228(3):129435-129475.

37. Jesintha, V., M. Mahalakshmi, A. Meera, B. Neppolian. 2024. Surface functionalized visible light-responsive yttrium orthovanadate for photocatalytic hydrogen production. Ceramics International50 (13):24626-24637.

38. Liu, K., Z. Yuan, H. Zhao, C. Shi, F. Zhao. 2023. Properties and Applications of Shape-Stabilized

Phase Change Energy Storage Materials Based on Porous Material Support—A review. Materials Today Sustainability 21(8):100336.

39. Khan, S., S. Mansoor, Z. Rafi, B. Kumari, A. Shoaib, M. Saeed, S. Alshehri, M. M. Ghoneim, M. Rahamathulla, U. Hani, F. Shakeel. 2022. A review on nanotechnology: Properties, applications, and mechanistic insights of cellular uptake mechanisms. Journal of Molecular Liquids 348 (9):118008.

40. Balouiri, M., M. Sadiki, L. K. Saad. 2015. Methods for in vitro evaluating antimicrobial activity: A review. Journal of Pharmaceutical Analysis 6 (2):71-79.

41. Taylor, R. S., N. P. Manandhar, G. H. N. Towers. 1995. Screening of selected medicinal plants ofNepal for antimicrobial activities. Journal of Ethnopharmacology 46 (3):153-159.

42. Jadaun, G. P. S., S. Rastogi, A. Kumar, J. Chauhan, S. K. Sharma, M. Kumar, P. K. Saini, R. Tiwari, R. S. Raghuvanshi. 2023. Ensuring the quality of medicines in India: An update on the development, modernization, and harmonization of drug standards in the Indian Pharmacopoeia. Saudi Pharmaceutical Journal 31(4):101825.